Journal of Radiation and Nuclear Applications
An International Journal

http://dx.doi.org/10.18576/jrna/080303

Investigation Of $(Pb_2O_3)_x(SnO_2)_{1-x}$ Photon Shielding Capabilities For Medical Radiation Application

Idris M. M.[1*], *Ewa M. K.*[1], *Iwa S. J.*[2], *Isah S. H.*[3], *and Suleiman A.*[1],

[1]Department of Physics, Faculty of Natural and Applied Sciences, Nasarawa State University Keffi, Nigeria.
[2]Department of Physics, Faculty of Science, Federal University of Technology Owerri, Imo State, Nigeria.
[3]Department of Mathematics, Faculty of Natural and Applied Sciences, Nasarawa State University Keffi, Nigeria.

Received: 02 Jul 2023, Revised: 04 Jul 2023, Accepted: 24 Aug. 2023.
Published online: 1 Sep 2023.

Abstract: This study investigates the photon shielding capabilities of $(Pb_2O_3)_x$ $(SnO_3)_{1-x}$ (x = 0, 0.2, 0.4, 0.6, 0.8 and 1 coded as C1, C2, C3, C4, C5 and C6 respectively) for medical radiation application. A numerical model was employed to determine the mass attenuation coefficients (MAC) of the mixture using WinXCOM computer program in the energy range of 0.020 – 20.0 MeV. The MAC values was used to calculate the linear attenuation coefficient (LAC), half-value layer (HVL), tenth value layer (TVL),mean free path (MFP), and effective atomic number (Z_{eff}). The results showed a smooth reduction in MAC value as the energy increases for all the mixtures. The maximum (minimum) MAC values were 17.087 (0.0336), 17.083 (0.0337), 17.074 (0.0339), 17.067 (0.0339), 17.060 (0.0341) and 17.054 (0.0342) cm^2/g for C1, C2, C3, C4, C5 and C6 respectively. The maximum Value of LAC was obtained at 0.02 MeV with values was obtained at 0.093, 0.098, 0.111, 0.118, 0.128 and 0.133 cm^{-1} respectively for C1, C2, C3, C4, C5, and C6 respectively. The LAC value are in the order of C6 > C5 > C4 > C3 > C2 > C1. The HVL, TVL, and MFP show similar pattern and are in the order of C1 > C2 > C3 > C4 > C5 > C6. The results indicates that SnO_2 showed the highest attenuation capabilities and declined as the Pb_2O_3 concentration increases. The study indicates that the attenuation of a shielding material can significantly be enhance by SnO_2 doping and can be deployed for medical radiation shielding application.

Keywords: WinXCOM software, Mass attenuation coefficient, Medical radiation shielding and SnO_2 and Pb_2O_3.

1 Introduction

Today, radiation sources are noteworthy materials for humanity since they have a wide range of application fields such as nuclear plants [1, 2], agriculture [3], food industry [4], medicine [5, 6], etc. Although the use of radioactive materials is inevitable for the aforementioned fields, as it pose health risk on humans [7, 8]. For this reason, researchers are particularly interested in developing new shielding materials in order to reduce the undesired effects of X and gamma rays on biological systems [9, 10, 11]. The remarkable increment in radioactivity risks of today's industrial world is required to the efficient design of shielding structures. Standard materials such as lead and concrete have been used to be shielding materials of ionizing radiation but however has some limitations [12, 13]. As such, it is necessary to improve the attenuating properties of lead by doping it with another material. This research assess the photon attenuation competence of Pb_2O_3 doped with SnO_2 using the winXCOM software.

2 Materials and Methods

The attenuation competence of Lead (II) oxide doped with Tin oxide were assessed. In this study, the attenuation parameters of $(Pb_2O_3)_x(TeO_2)_{1-x}$ for x = 0, 0.2, 0.4, 0.6, 0.8, and 1 coded as C1, C2, C3, C4, C5 and C6 respectively, were determined. The mass attenuation coefficient (MAC) of the mixture were determined using winXCOM software program installed in a laptop computer. The XCOM code is a database for calculating mass attenuation coefficients at different photon energies [14-16]. Linear attenuation coefficients (LAC) were calculated by multiplying the obtained theoretical MAC value by the density of the mixtures. LAC is one of the most important parameter that describe the gamma rays penetrating process which depends on the energy of incident photons and atomic

*Corresponding author e-mail: idrismustapham@nsuk.edu.ng

number or effective atomic number of the target. It is also considered as the main factor for the derivation of other shielding parameters (Singh & Badiger, 2013). The linear attenuation coefficient is related to the mass attenuation coefficient as [15, 17]:

$$\mathrm{MAC} = \frac{\mathrm{LAC}}{\rho} \qquad 1$$

where ρ represents the density of the absorbing medium. It has the dimensions of area per unit mass (cm^2g^{-1}). The half value layer and mean free path are important related shielding parameters were calculated using [14, 15]:

$$\mathrm{HVL} = \frac{\ln 2}{\mathrm{LAC}} \qquad 2$$

and

$$\mathrm{MFP} = \frac{1}{\mathrm{LAC}} \qquad 3$$

The HVL and MFP reflect the necessary thickness that should be used to attenuate gamma rays or x-rays by half and a factor of e, respectively.

3 Results and Discussion

Table 1 shows the chemical compositions and densities of the doped compounds studied. The pot of mass attenuation coefficient (MAC) and linear attenuation coefficient (LAC) obtained in the energy range of 0.02–20MeV using the WinXCOM program is shown in Figure 1 and 2 respectivey. The MAC versus photon energy spectra of the mixtures (C1 - C6) are shown in Figure 1. The MAC values shows a smooth reduction as the energy increases for all the mixtures. The decrease in MAC values from 0.020 to 0.09 MeV was very drastic compare to rest of energy spectrum. This observed sharp declined in MAC values is due to dominance of photoelectric interaction cross section (PI). The maximum (minimum) MAC values were 17.087 (0.0336), 17.083 (0.0337), 17.074 (0.0339), 17.067 (0.0339), 17.060 (0.0341) and 17.054 (0.0342) cm^2/g for C1, C2, C3, C4, C5 and C6 respectively. Throughout the considered energy range, the relative values of MAC for the mixtures follow the order: C1< C2 < C3 < C4 < C5 < C6. The increase in the mass density of the mixture brought about by the increase in the SnO_2 concentration is a major factor responsible for the observed increase in MAC values. The trend of LAC values follows similarly to that of the MAC values. However, the relative difference in the linear attenuation co-efficient is higher than that observed for MAC. This is due to the difference in mass density of the mixtures [18-21].

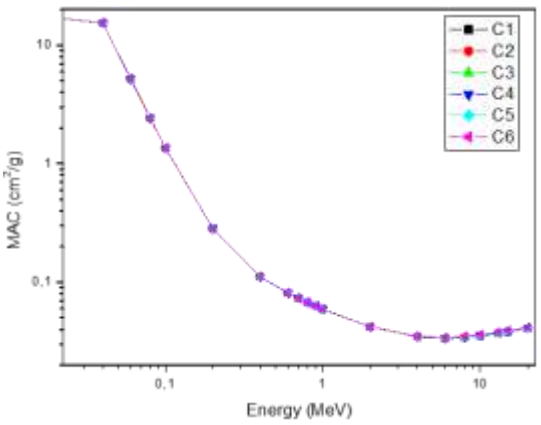

Fig. 1: Mass Attenuation Coefficient spectra of $(Pb_2O_3)_x$ $(SnO_3)_{1-x}$ samples.

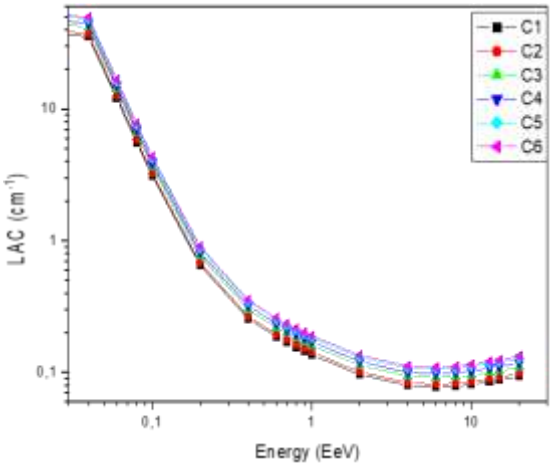

Fig. 2: Linear Attenuation Coefficient spectra of $(Pb_2O_3)_x$ $(SnO_3)_{1-x}$ samples.

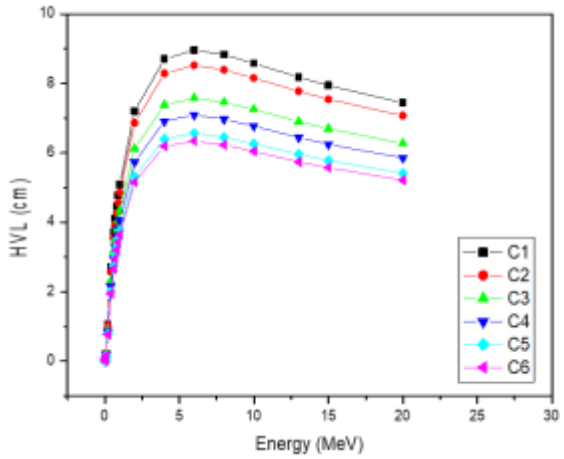

Fig. 3: Half Value Layer spectra of $(Pb_2O_3)_x$ $(SnO_3)_{1-x}$ samples.

Table 1: Chemical compositions and densities of the Pb_2O_3 doped SnO_3 samples.

S/N	Sample Code	Chemical Composition	Density (g/cm^3)
1.	C1	Pb_2O_3	2.13
2.	C2	$0.8Pb_2O_3$-$0.2SnO_3$	2.30
3.	C3	$0.6Pb_2O_3$-$0.4SnO_3$	2.85
4.	C4	$0.4Pb_2O_3$-$0.6SnO_3$	2.95
5.	C5	$0.2Pb_2O_3$-$0.8SnO_3$	3.10
6.	C6	SnO_3	3.25

Table 2: The MAC values of Pb_2O_3 doped SnO_3 mixture in the energy range of 0.020 - 20 MeV by WinXCOM software.

S/N	Energy MeV	C1	C2	C3	C4	C5	C6
1. `	2.00E-02	1.71E+01	1.71E+01	1.71E+01	1.71E+01	1.71E+01	1.71E+01
2.	4.00E-02	1.54E+01	1.54E+01	1.54E+01	1.55E+01	1.55E+01	1.55E+01
3.	6.00E-02	5.21E+00	5.22E+00	5.23E+00	5.23E+00	5.24E+00	5.25E+00
4.	8.00E-02	2.42E+00	2.42E+00	2.43E+00	2.43E+00	2.43E+00	2.43E+00
5.	1.00E-01	1.35E+00	1.35E+00	1.36E+00	1.36E+00	1.36E+00	1.36E+00
6.	2.00E-01	2.83E-01	2.83E-01	2.83E-01	2.83E-01	2.83E-01	2.83E-01
7.	4.00E-01	1.11E-01	1.11E-01	1.11E-01	1.11E-01	1.12E-01	1.12E-01
8.	6.00E-01	8.10E-02	8.11E-02	8.11E-02	8.12E-02	8.12E-02	8.13E-02
9.	7.00E-01	7.33E-02	7.33E-02	7.34E-02	7.34E-02	7.35E-02	7.35E-02
10.	8.00E-01	6.75E-02	6.76E-02	6.76E-02	6.76E-02	6.77E-02	6.77E-02
11.	9.00E-01	6.30E-02	6.30E-02	6.30E-02	6.31E-02	6.31E-02	6.31E-02
12.	1.00E+00	5.92E-02	5.93E-02	5.93E-02	5.93E-02	5.94E-02	5.94E-02
13.	2.00E+00	4.19E-02	4.19E-02	4.19E-02	4.20E-02	4.20E-02	4.20E-02
14.	4.00E+00	3.46E-02	3.47E-02	3.48E-02	3.48E-02	3.49E-02	3.50E-02
15.	6.00E+00	3.36E-02	3.37E-02	3.38E-02	3.40E-02	3.41E-02	3.42E-02
16.	8.00E+00	3.41E-02	3.43E-02	3.44E-02	3.45E-02	3.46E-02	3.48E-02
17.	1.00E+01	3.51E-02	3.53E-02	3.54E-02	3.56E-02	3.57E-02	3.59E-02
18.	1.30E+01	3.68E-02	3.70E-02	3.72E-02	3.74E-02	3.75E-02	3.77E-02
19.	1.50E+01	3.80E-02	3.81E-02	3.83E-02	3.85E-02	3.87E-02	3.89E-02
20.	2.00E+01	4.05E-02	4.07E-02	4.09E-02	4.11E-02	4.13E-02	4.16E-02

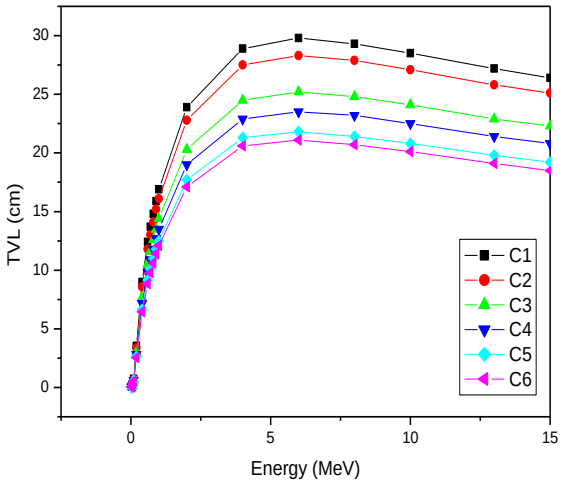

Fig. 4: Tenth Value Layer spectra of $(Pb_2O_3)_x$ $(SnO_3)_{1-x}$ samples.

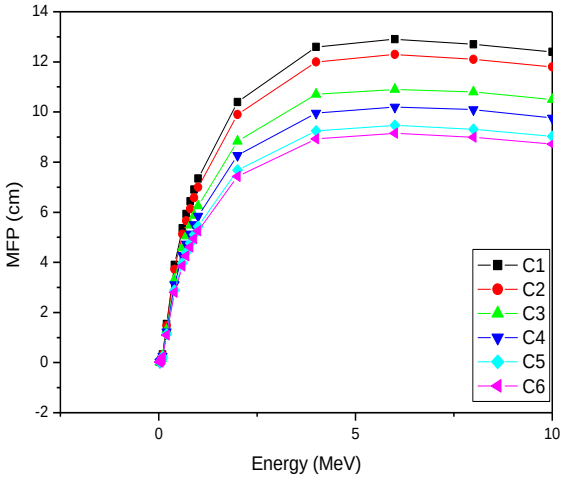

Fig. 5: Mean Free Path spectra of $(Pb_2O_3)_x$ $(SnO_3)_{1-x}$ samples.

Figure 3, 4, and 5 shows the plot of half value layer (HVL), tenth value layer (TVL), and mean free path (MFP) respectively. The HVL and TVL generally increase with photon energy for all the mixtures, an indication that higher energy photons are more penetrating hence; more thickness of absorbing materials is required to absorb them. The trend of HVL and TVL values of the mixtures is inverse to that of LAC, hence, the highest values of TVL was obtained for C1. This is because the mixture sample has the least density due to zero SnO_3 content. The MFP increase with photon energy which affirms that higher energy photons travel further in the mixture due to reduced interaction cross sections of the process leading to absorption.

4 Conclusions

In this study, the photon shielding capabilities of $(Pb_2O_3)_x$ $(SnO_3)_{1-x}$ (x = 0, 0.2, 0.4, 0.6, 0.8 and 1 coded as C1, C2, C3, C4, C5 and C6 respectively) was investigated. A numerical model was employed to determine the mass attenuation coefficients (MAC) of the mixture using WinXCOM computer program in the energy range of 0.020 – 20.0 MeV. The MAC values was used to calculate the linear attenuation coefficient (LAC), half-value layer (HVL), tenth value layer (TVL),mean free path (MFP), and effective atomic number (Z_{eff}). The results showed a smooth reduction in MAC value as the energy increases for all the mixtures. The LAC value are in the order of C6 > C5 > C4 > C3 > C2 > C1. The HVL, TVL, and MFP show similar pattern and are in the order of C1 > C2 > C3 > C4 > C5 > C6. The results indicates that SnO_2 showed the highest attenuation capabilities and declined as the Pb_2O_3 concentration increases. The study indicates that the attenuation of a shielding material can significantly be enhance by SnO_2 doping and can be deployed for medical radiation shielding application.

Conflict of Interest

The authors declares that there was no competing interest.

Reference

[1] Lee, U., Lee, C., Kim, M. & Kim, H. R. (2019). Analysis of the influence of nuclear facilities on environmental radiation by monitoring the highest nuclear power plant density region, Nucl. Eng. Technol. 51(4) 1626–1632.

[2] Okuno, Y., Okubo, N. & Imaizumi, M. (2019). Application of InGaP space solar cells for a radiation dosimetry at high dose rates environment of Fukushima Daiichi nuclear power plant, J. Nucl. Sci. Technol. 56(1) 851–858.

[3] Pragya, D. K., Das, V. K., Sehgal, T. K. & Das, J. (2018). Mukherjee, Evaluation of conservation agriculture practices for radiation interception and biophysical properties in rice-mustard cropping system, Mausam 69(1) 607–614.

[4] Barba, F. J., Gavahian, I. Es, M., Zhu, Z. Z., Chemat, F. Lorenzo, J. M. & Khaneghah, A. M. (2019). Solar radiation as a prospective energy source for green and economic processes in the food industry: from waste biomass valorization to dehydration, cooking, and baking, J. Clean. Prod. 220(4) 1121–1130.

[5] Damulira, E., Yusoff, M .N. S., Omar, A. F. & Taib, N. H. M. (2019). A review: photonic devices used for Dosimetry in medical radiation, Sens.-Basel 19(4) 2226.

[6] Jin, Y., (2019). Low-cost and active control of radiation of wearable medical health device for wireless body area network, J. Med. Syst. 43 137.

[7] Azman, R. R., Shah, M. N. M., K. H. (2019). Ng, Radiation safety in emergency medicine: balancing the benefits and risks, Korean J. Radiol. 20 399–404.

[8] Boice, J. D. (2019). Welcome to the 54th annual meeting of the National Council on radiation protection and measurements: radiation protection responsibility in medicine, Health Phys. 116(4) 111–116.

[9] RM. El-Sharkawy., KS. Shaaban, R. Elsaman., EA. Allam., A. El-Taher., ME. Mahmoud, ME., Investigation of mechanical and radiation shielding characteristics of novel glass systems with the

*Corresponding author e-mail: idrismustapham@nsuk.edu.ng

composition xNiO-20ZnO-60B2O3-(20-x) CdO based on nanometal oxides. Journal of Non-Crystalline Solids. 528, 119754. 2020.

[10] RM. El-Sharkawy., EA. Allam., A. El-Taher., ER. Shaaban. and ME. Mahmoud., Synergistic Effect of Nano-bentonite and Nano cadmium Oxide Doping Concentrations on Assembly, Characterization and Enhanced Gamma-Rays Shielding Properties of Polypropylene Ternary Nanocomposites. International Journal of Energy Research. 45 (6), 8942-8959. 2021.

[11] YB Saddeek, KHS Shaaban, R Elsaman, A. El-Taher, TZ Amer., Attenuation-density anomalous relationship of lead alkali borosilicate glasses. Radiation Physics and Chemistry 150, 182-188. 2018.

[12] Hassan, H. E., Badran, H. M., Aydarous, A. & Sharshar, T. (2015). Studying the effect of nano lead compounds additives on the concrete shielding properties for γ-rays, Nucl. Instrum. Meth. B 360(1) 81–89.

[13] HMH Zakaly, A. Ashry, A. El-Taher, AGE Abbady, EA Allam, ...Role of novel ternary nanocomposites polypropylene in nuclear radiation attenuation properties: In-depth simulation study. Radiation Physics and Chemistry 188, 109667. 2021.

[14] A El-Taher, HMH Zakaly, M Pyshkina, EA Allam, RM El-Sharkawy, ...A comparative Study Between Fluka and Microshield Modeling Calculations to study the Radiation-Shielding of Nanoparticles and Plastic Waste composites. Zeitschrift für anorganische und allgemeine Chemie 647 (10), 1083-1090. 2021.

[15] Idris M. M., Atimga B. J. and Sulayman M. B. Photon Shielding Characterization of SiO2-PbO-CdOTiO2 Glasses for Radiotheraphy Shielding Application. Asian Journal of Research and Reviews in Physics, 4(4): 32-38, 2021

[16] Baqiah, H., Ibrahim, M. H., Abdi, S. A., & Halim. (2013). Electrical transport, microstructure and optical properties of Cr-doped In2O3 thin film prepared by sol–gel method, J. Alloy. Compd. 575(4) 198–206.

[17] EA Allam, RM El-Sharkawy, A. El-Taher, ER Shaaban, EES Massoud, Mohamed E Mahmoud., Enhancement and optimization of gamma radiation shielding by doped nano HgO into nanoscale bentonite. Nuclear Engineering and Technology 54 (6), 2253-2261, 2022.

[18] A. El-Taher., HM. Mahmoud and Adel G.E Abbady,. Comparative Study of Attenuation and Scattering of Gamma –Ray through Two Intermediate Rocks. Indian Journal of Pure & Applied Physics, 45. 2007.

[19] A. El-Taher., AM, Ali., YB. Saddeek., R. Elsaman., H. Algarni., HS. Shaaban., TZ. Amer., Gamma ray shielding and structural properties of iron alkali alumino-phosphate glasses modified by PbO. Radiation Physics and Chemistry, 165, 108403. 2019.

[20] ME. Mahmoud, RM. El-Sharkawy., EA. Allam, R. Elsaman., A. El-Taher., Fabrication and characterization of phosphotungstic acid-Copper oxide nanoparticles-Plastic waste nanocomposites for enhanced radiation-shielding. Journal of Alloys and Compounds 803, 768-777. 2019.

[21] RM, El-Sharkawy., EA. Allam., A. El-Taher., R. Elsaman., EE. Massoud., ME. Mahmoud,., Synergistic effects on gamma-ray shielding by novel light-weight nanocomposite materials of bentonite containing nano Bi2O3 additive. Ceramics International 48 (5), 7291-7303. 2022.